

## MIXED-MODE IMPEDANCE AND REFLECTION COEFFICIENT OF TWO-PORT DEVICES

T. Carrasco<sup>1, \*</sup>, J. Sieiro<sup>1</sup>, J. M. Lopez-Villegas<sup>1</sup>, N. Vidal<sup>1</sup>,  
R. Gonzalez-Echevarria<sup>2</sup>, and E. Roca<sup>2</sup>

<sup>1</sup>Department of Electronics, Faculty of Physics, University of Barcelona, Marti i Franques 1, Barcelona 08028, Spain

<sup>2</sup>Institute of Microelectronics of Seville, CSIC and University of Seville Avda. Americo Vespucio s/n, Isla de la Cartuja, Seville 41092, Spain

**Abstract**—From the point of view of mixed-mode scattering parameters,  $S_{mm}$ , a two-port device can be excited using different driving conditions. Each condition leads to a particular set of input reflection and input impedance coefficient definitions that should be carefully applied depending on the type of excitation and symmetry of the two-port device. Therefore, the aim of this paper is to explain the general analytic procedure for the evaluation of such reflection and impedance coefficients in terms of mixed-mode scattering parameters. Moreover, the driving of a two-port device as a one-port device is explained as a particular case of a two-port mixed-mode excitation using a given set of mixed-mode loads. The theory is applied to the evaluation of the quality factor,  $Q$ , of symmetrical and non-symmetrical inductors.

### 1. INTRODUCTION

Currently, most of the RFICs are designed to work in differential configuration due to noise immunity. In fact, the majority of the receiver chipsets available in today's market, as well as some of the components that conform them, are fully differential [1, 2]. Obviously, it implies that the figures of merit of these devices are better expressed in terms of mixed-mode scattering parameters ( $S_{mm}$ ), which were first introduced by Bockelman and Eisenstadt [3, 4]. In spite of their widespread use in RFIC design, there is still some misunderstanding about how the differential (common)-mode input impedance  $Z_d$  ( $Z_c$ )

---

*Received 29 May 2012, Accepted 18 July 2012, Scheduled 20 August 2012*

\* Corresponding author: Carrillo Tomas Carrasco (tcarrasco@el.ub.es).

must be calculated in terms of  $S_{mm}$  when a two-port is seen as a one-port device. Thus, it is usually found that the differential reflection coefficient  $\Gamma_d$  of a two-port device is assumed to be  $S_{dd}$  [5–8]. Therefore, the differential input impedance is calculated using the following bilinear impedance transformation

$$Z_{dd} = 2Z_0 \frac{1 + S_{dd}}{1 - S_{dd}} \quad (1)$$

where  $2Z_0$  is the differential surge impedance. Certainly,  $Z_{dd}$  in (1) coincides with the differential term of the mixed-mode  $Z$ -parameter matrix of a two-port device; however, as it has been previously mentioned in [9] and [10], a close look to (1) reveals that such expression only matches with  $Z_d$  (i.e.,  $Z_d = Z_{dd}$ ) for fully symmetrical two-port devices. For non-symmetrical devices and taking into account the definition of  $S_{dd}$ , (1) neglects any conversion to a reflected common-mode power wave. Then, special care must be taken when using (1) as an equivalent expression to  $Z_d$ . For instance, the evaluation of the quality factor  $Q$  using the next definition

$$Q = \frac{\text{Im}\{Z_{dd}\}}{\text{Re}\{Z_{dd}\}} \quad (2)$$

should be only applied to symmetrical topologies. For non-symmetrical inductors, e.g., spiral inductors, (2) wrongly estimates  $Q$ , due to the fact that the component boundary conditions are wrongly set, thus the common-mode conversion is completely dismissed. A similar misunderstanding can be pointed out when  $Z_{cc}$  is directly related to  $Z_c$ ; in this case, any conversion to differential-mode is not considered.

To avoid the former problem, [10] and [11] transform the description of the two-port device from  $S$ -parameters to  $Z$ -parameters. Then, a floating current or voltage source is applied between the input ports of the device, instead of normalized power waves. These boundary conditions lead to a different input impedance definition which can be transformed back to  $S$ -parameters. Besides, an equivalent solution is found in [12] and [13] by means of applying the same floating signal sources to the two-port, but such boundary conditions are straightly expressed in terms of  $S$ -parameters, instead of transforming to  $Z$ -parameters. In both cases, the input impedance found shows the non-symmetrical response of the device. However, up to the author's knowledge no procedure expressing  $\Gamma_d$  ( $\Gamma_c$ ) or  $Z_d$  ( $Z_c$ ) in terms of  $S_{mm}$  has been yet proposed. Even more, all previous cases must be understood as particular cases of a general expression based on the definitions of mixed-mode scattering parameters and loads.

Within this framework, the rest of this paper is devoted to extend the theory of mixed-mode scattering parameters not only to

symmetrical devices, but to non-symmetrical or actual devices. For this reason, in Section 2, a general expression of  $\Gamma_d(\Gamma_c)$  will be obtained which resembles the well-known expressions of  $\Gamma_{in}(\Gamma_{out})$  for a single-ended two-port device. Such definitions will allow to obtain  $Z_d(Z_c)$  in terms of  $S_{mm}$ . In Section 3, it is shown that former particular cases of the driving of a two-port device are reduced to the application of a short, open and matched mixed-mode load conditions on the general expression of  $\Gamma_d(\Gamma_c)$ . As a practical case in Section 4, an adequate definition of  $Q$  will be obtained, by means of  $Z_d$ , that allows the direct comparison between symmetrical and non-symmetrical inductors. Finally, the conclusions of this work are presented in Section 5.

## 2. INPUT REFLECTION COEFFICIENT OF A TWO-PORT DEVICE

When attempting to calculate  $\Gamma_d(\Gamma_c)$ , it is useful to keep in mind the definition of the input(output) reflection coefficient  $\Gamma_{in}(\Gamma_{out})$  of a two-port device. As it can be seen in Fig. 1,  $\Gamma_{in}$  is defined as the quotient between the incident power wave  $a_1$  and the reflected power wave  $b_1$  at the input port  $P_1$ , when a load  $Z_L$  has been connected to the output port. Besides,  $\Gamma_{out}$  is the reflection coefficient towards the output port  $P_2$ , when a source impedance  $Z_S$  has been connected to the input port [14, 15]. Due to the fact that there is a linear transformation between  $S$  and  $S_{mm}$ , i.e.,  $S = M^{-1}S_{mm}M$  [16], the two-port network in Fig. 1 can be represented as a two-port device where the input port and the output port have been substituted by a differential and common-mode ports. At this point,  $\Gamma_d(\Gamma_c)$  can be correctly defined by analogy to  $\Gamma_{in}(\Gamma_{out})$ . Consequently,  $\Gamma_d(\Gamma_c)$  is the input reflection coefficient of a two-port device when exciting with a differential (common)-mode power wave meanwhile the two-port device is loaded with a common

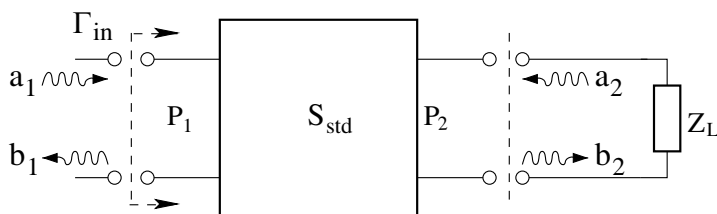


**Figure 1.** Input reflection coefficient of a two-port device in standard  $S$ -parameters.

(differential)-mode load.

### 2.1. Differential-mode Input Reflection Coefficient, $\Gamma_d$

Figure 2 shows how a differential power wave  $a_d$  is launched towards a two port device meanwhile a common-mode impedance  $Z_L^c$  is connected to the common-mode port.  $S_{mm}$  relates the incident and reflected differential and common-mode power waves by

$$\begin{pmatrix} b_d \\ b_c \end{pmatrix} = \begin{pmatrix} S_{dd} & S_{dc} \\ S_{cd} & S_{cc} \end{pmatrix} \begin{pmatrix} a_d \\ a_c \end{pmatrix}. \quad (3)$$

In this case, the two-port scatters back two power waves  $b_d$  and  $b_c$ . The common-mode reflected wave  $b_c$  reaches the common-mode load  $Z_L^c$ , which reflects a common-mode wave  $a_c$ . Thereby, it can be written the following relation

$$a_c = \Gamma_L^c b_c \quad (4)$$

where  $\Gamma_L^c$  is the reflection coefficient associated with  $Z_L^c$ . Replacing (4) in (3) and after some algebra,  $\Gamma_d$  is expressed as follows

$$\Gamma_d = \frac{S_{dd} - |S| \Gamma_L^c}{1 - S_{cc} \Gamma_L^c}. \quad (5)$$

Notice that, whenever a two-port is completely symmetric and balanced (i.e.,  $S_{11} = S_{22}$  and  $S_{12} = S_{21}$ , which lead to  $S_{dc} = S_{cd} = 0$  and  $|S| = S_{dd} S_{cc}$ ),  $\Gamma_d$  is equal to  $S_{dd}$  irrespective of the connected load  $Z_L^c$ . In this case, as it has been previously mentioned,  $Z_d$  matches  $Z_{dd}$ .

It is also interesting to rewrite (4) as a function of the incident power wave  $a_1$  and  $a_2$  at each port referred to the common ground. From [3],  $a_{d(c)}$  and  $b_{d(c)}$  read as

$$\begin{aligned} a_{d(c)} &= \frac{1}{\sqrt{2}} (a_1 \mp a_2) \\ b_{d(c)} &= \frac{1}{\sqrt{2}} (b_1 \mp b_2) \end{aligned} \quad (6)$$

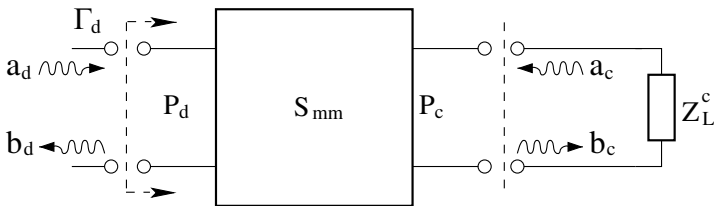


**Figure 2.** Differential-mode reflection coefficient of a two-port device in mixed-mode  $S$ -parameters.

where the upper and lower signs hold for the differential and common-mode, respectively. Substituting (6) in (4), the following relation is obtained

$$a_1 = -a_2 + \sqrt{2}\Gamma_L^c b_c. \tag{7}$$

Note that even though a differential power wave  $a_d$  is launched through the two-port device,  $a_1$  equals  $-a_2$  only in two cases: 1)  $\Gamma_L^c = 0$ , i.e., the common-mode load is a matched load; 2)  $b_c = 0$ , i.e., the two-port is purely balanced. For the remaining cases,  $a_1$  differs from  $-a_2$  due to the fact that a common-mode power wave  $a_c$  is scattered back by the common-mode load.

Keeping in mind the existing linear transformation between  $S$  and  $S_{mm}$  parameters, notice the duality of (5) when it is compared with the  $\Gamma_{in}$  ( $\Gamma_{out}$ ) expression of the single-ended analysis of a two-port device

$$\begin{aligned} \Gamma_{in} &= \frac{S_{11} - |S|\Gamma_L}{1 - S_{22}\Gamma_L} \\ \Gamma_{out} &= \frac{S_{22} - |S|\Gamma_S}{1 - S_{11}\Gamma_S}. \end{aligned} \tag{8}$$

By means of this comparison, one realizes that, as in the single-ended case, three standard loads can be defined: a matched load ( $\Gamma_L^c = 0$ ), an open-circuit ( $\Gamma_L^c = 1$ ) and a short-circuit ( $\Gamma_L^c = -1$ ). Notice that, each of these cases results in a different boundary condition when substituting  $\Gamma_L^c = 0, 1, -1$  in (4) as it will be analyzed in Section 3.

### 2.2. Common-mode Input Reflection Coefficient, $\Gamma_c$

Whenever a common-mode power wave  $a_c$  is launched towards a two-port device, as it can be seen in Fig. 3, two power waves,  $b_d$  and  $b_c$  are scattered back. Now,  $b_d$  reaches the differential load,  $Z_L^d$ , which reflects a differential-mode normalized power wave  $a_d$ . The relationship established between  $a_d$  and  $b_d$  through  $Z_L^d$  is

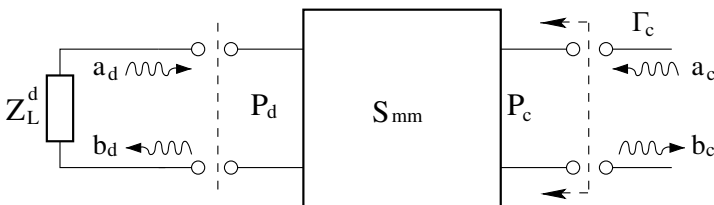


**Figure 3.** Common-mode reflection coefficient of a two-port device in mixed-mode  $S$ -parameters.

$$a_d = \Gamma_L^d b_d \quad (9)$$

wherein  $\Gamma_L^d$  is the reflection coefficient of the differential-mode load. A dual expression of (5) can be written when substituting (9) in (3),

$$\Gamma_c = \frac{S_{cc} - |S| \Gamma_L^d}{1 - S_{dd} \Gamma_L^d}. \quad (10)$$

Notice that, when the two-port is symmetric and balanced (i.e.,  $S_{dc} = S_{cd} = 0$  and  $|S| = S_{dd} S_{cc}$ ),  $\Gamma_c$  equals  $S_{cc}$  irrespective of the connected load. As it has been previously mentioned, only in this case  $Z_c$  matches  $Z_{cc}$ .

By replacing (6) in (9),  $a_1$  relates to  $a_2$  as follows

$$a_1 = a_2 + \sqrt{2} \Gamma_L^d b_d. \quad (11)$$

Therefore, even when a common-mode power wave  $a_c$  is launched through the two-port device,  $a_1$  equals  $a_2$  only in two cases: 1)  $\Gamma_L^d = 0$ , i.e., the differential-mode load is a matched load; or 2)  $b_d = 0$ , i.e., the two port is ideally balanced. Otherwise,  $a_1$  differs from  $a_2$ . This is due to the fact that a differential-mode power wave  $a_d$  is reflected back by the differential-mode load.

Equation (10) represents the dual case of (5). Therefore, three differential mixed-mode load conditions can be defined by means of  $\Gamma_L^d = 0, 1, -1$ .

### 3. MIXED-MODE DRIVING CONDITIONS

Three driving conditions can be defined which lead to different boundary conditions for a two-port device and different expressions of  $\Gamma_d$  ( $\Gamma_c$ ). In order to explore these driving conditions, it is very illustrative to think about the theoretical realization of a true mixed-mode VNA as the one in Fig. 4. Notice that, in contrast to the two-port device in Fig. 3, the device represented in Fig. 4 is a physical realization where the two input ports and the existing common-ground can be associated to either a single-ended or a mixed-mode representation. Actually, the physical realization of a pure-mode VNA (PMVNA) is rather difficult and, even though some works have been conducted toward its consecution [17, 18], current multi-port VNAs implement Bockelman's formulation to display  $S_{mm}$ . In fact, a commercial PMVNA is not yet available.

It is also important to notice that the DUT is normally connected to the PMVNA by means of a pair of coupled transmission lines and a ground reference which allows the propagation of differential and common-mode power waves. However, as it has been previously

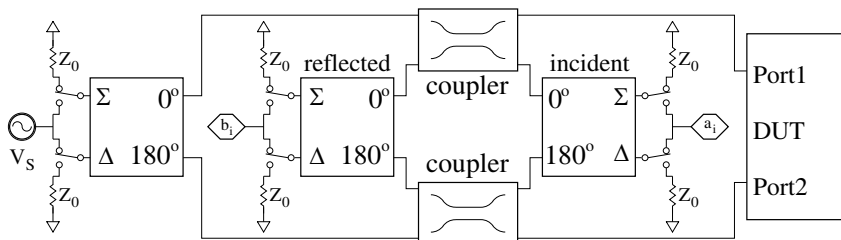


Figure 4. Pure-mode vector network analyzer.

demonstrated in [3], if the even and odd-mode characteristic impedance are chosen to be equal, such reference coupled lines can be considered uncoupled transmission lines. Even more, as it is also mention, there is not restriction for the length of the reference lines, thus zero length transmission lines can be defined and (6) still holds on.

### 3.1. Matched Load $\Gamma_L^{d(c)}=0$

Whenever a power wave is launched from the  $V_s$  generator in Fig. 4, a switchable  $0^\circ/180^\circ$  hybrid generates either a differential  $a_d$  or common-mode  $a_c$  power waves. These incident waves can be measured accordingly the  $0^\circ/180^\circ$  input at the incident wave hybrid. When the selected power wave reaches the DUT, the incident power wave is scattered back, as well as an opposite mode wave is generated due to the asymmetry of the two-port device. Both modes can be measured by setting the switchable  $0^\circ/180^\circ$  reflected wave hybrid. It is important to notice that whenever one mode is selected, the opposite mode is connected to its surge impedance  $2Z_0$  or  $Z_0/2$  through each hybrid, thus non scattered wave from the loads is allowed. This assumption is similar to connect  $Z_0$  at the opposite port with respect to the one that is being measured when the measure of  $S_{11}$  or  $S_{22}$  is done by means of a classical VNA. Assuming the condition that the incoming wave is  $a_d$ , and keeping in mind that  $\Gamma_L^c = 0$ , from (5)  $\Gamma_d$  reads as

$$\Gamma_d = S_{dd}. \tag{12}$$

In this case, from (4)  $a_c$  is equal to zero. Thus,  $a_1$  equals  $-a_2$ . Only when the reflected power wave is absorbed in the common-mode load, the normalized power waves ingoing into the two-port device are equal in magnitude and opposite sign, thus they are pure differential signals. Besides, whenever it is assumed that  $a_1 = -a_2$ , this condition always leads to  $\Gamma_d = S_{dd}$ , even though  $a_c$  differs actually from zero in an actual measurement setup. Then, it is not surprising that, when attempting to calculate  $\Gamma_d$  by means of a  $0^\circ/180^\circ$  hybrid or an equivalent device

which supposedly generates the boundary condition  $a_1 = -a_2$ ,  $\Gamma_d$  is misunderstood as  $S_{dd}$  and any common-mode conversion is directly dismissed.

In order to calculate  $Z_d$ , the bilinear transformation (1) is valid and  $Z_d$  is equal to  $Z_{dd}$ .

Likewise, if  $a_c$  is launched by the power generator  $V_s$ , and  $\Gamma_L^d = 0$  is selected at the hybrids, from (10)  $\Gamma_c$  reads as

$$\Gamma_c = S_{cc}. \quad (13)$$

From (9)  $a_d$  is equal to zero, thus  $a_1$  equals  $a_2$ . Therefore, if the boundary condition  $a_1 = a_2$  is assumed, it directly leads to obtain that  $\Gamma_c = S_{cc}$ , although  $a_d$  could actually differ from zero. Then, when  $\Gamma_c$  is calculated by means of a device which supposedly generates  $a_1 = a_2$ ,  $\Gamma_c$  is misunderstood as  $S_{cc}$  and any differential-mode conversion is dismissed. In this case,  $Z_c$  can be calculated by means of the bilinear transformation

$$Z_c = \frac{Z_0}{2} \frac{1 + S_{cc}}{1 - S_{cc}} \quad (14)$$

where  $Z_0/2$  is the surge impedance for the common-mode.

Although the normal operation of a PMVNA is the one previously described, the ports  $\Sigma$  and  $\Delta$  at the hybrids, where the differential or common-mode load are connected, can be left open or shorted. In these cases, a scattered wave is allowed and  $\Gamma_L^{d(c)}$  equals 1 or  $-1$  respectively.

### 3.2. $\Gamma_d$ when $\Gamma_L^c=1$

Replacing  $\Gamma_L^c = 1$  in (5),  $\Gamma_d$  results as follows

$$\Gamma_d = \frac{S_{dd} - |S|}{1 - S_{cc}}. \quad (15)$$

As it has been previously mention, if the device is symmetric (i.e.,  $S_{cd} = S_{dc} = 0$  and  $|S| = S_{dd}S_{cc}$ ),  $\Gamma_d$  equals  $S_{dd}$ . It is also interesting to notice that if the device is also floating, as the balanced antenna discussed in [10, 19] (i.e.,  $S_{cc} = 1$  and  $|S| = S_{dd}$ ),  $\Gamma_d$  calculated by means of (15) results in an indetermination. This result was previously mentioned in [20], but now by using (5) the indetermination is naturally solved and  $\Gamma_d$  results in  $S_{dd}$ .

Once  $\Gamma_d$  has been obtained,  $Z_d$  can be easily calculated by means of the bilinear transformation

$$Z_d = 2Z_0 \frac{1 + \Gamma_d}{1 - \Gamma_d}. \quad (16)$$

However, it is also very illustrative to obtain  $Z_d$  by using circuit theory, i.e., writing the voltage and current signals at each port in



terms of mixed-mode  $S$ -parameters. Proceeding in this way, both  $S_{mm}$  and circuit theory are shown to be mathematically equivalent and, additionally, the goodness of the bilinear impedance transformation is highlighted.

Thus, when  $\Gamma_L^c = 1$ , (7) can be rewritten as

$$a_1 = -a_2 + \sqrt{2}b_c. \tag{17}$$

As it has been previously mentioned,  $a_1$  differs from  $a_2$  except when the two port is purely symmetric. Otherwise, replacing  $b_c$  by (6) and by means of the following expressions [3]

$$\begin{aligned} V_i &= \sqrt{Z_0} (a_i + b_i) \\ I_i &= \frac{1}{\sqrt{Z_0}} (a_i - b_i), \end{aligned} \tag{18}$$

(17) can be written as  $I_1 = -I_2$ . It means that the normalized power waves can be replaced by a floating current source as it is shown in Fig. 5 and the result is equivalent to (15). Consistently, the condition  $I_1 = -I_2$  implies that there is no common-mode current flowing into the device; thus, from the point of view of the common-mode, it can be seen as an open load, i.e.,  $\Gamma_L^c = 1$ .

In order to calculate  $Z_d$ , both currents can be expressed in terms of  $S$ -parameters as follows

$$\begin{aligned} I_1 &= \frac{1}{\sqrt{Z_0}} (a_1 - b_1) = \frac{1}{\sqrt{Z_0}} [(1 - S_{11}) a_1 - S_{12} a_2] \\ I_2 &= \frac{1}{\sqrt{Z_0}} (a_2 - b_2) = \frac{1}{\sqrt{Z_0}} [-S_{21} a_1 + (1 - S_{22}) a_2]. \end{aligned} \tag{19}$$

Thus,  $a_2$  can be written in terms of  $a_1$ :

$$a_2 = -\frac{a_1 (-1 + S_{11} + S_{21})}{-1 + S_{22} + S_{12}} = -a_1 \frac{S_{cc} + S_{cd} - 1}{S_{cc} - S_{cd} - 1}. \tag{20}$$

Note that for a symmetric and reciprocal two-port device (i.e.,  $S_{dc} = S_{cd} = 0$ ), (20) results in  $a_2 = -a_1$ . Otherwise, the ingoing waves are different at each port, and such difference depends on  $S_{cc}$  and  $S_{cd}$  which convey a common-mode conversion. Now, by means of (20), the voltage and currents at each node of the DUT can be rewritten as a function of  $a_1$  as

$$V_i = \sqrt{Z_0} a_1 \left\{ \pm \frac{S_{dd} - S_{cc} + 1 - |S|}{1 - S_{cc} + S_{cd}} + \frac{2S_{cd}}{1 - S_{cc} + S_{cd}} \right\} \tag{21}$$

$$I_1 = -I_2 = \frac{1}{\sqrt{Z_0}} a_1 \frac{S_{dd} - S_{cc} - 2S_{cd} + 1 - |S|}{1 - S_{cc} + S_{cd}} \tag{22}$$

where in (21) the upper and lower signs hold for port 1 and port 2, respectively. As a matter of fact, only when the two-port device is symmetric, (21) results in  $V_1 = -V_2$ .

From (21) and (22),  $V_d = V_1 - V_2$  and  $I_d = I_1 = -I_2$  can be calculated and, since  $Z_d$  is  $V_d/I_d$ , it reads as follows

$$Z_d = Z_0 \left( \frac{1 + S_{dd} + S_{dc}}{1 - S_{dd} - S_{cd}} + \frac{(1 + S_{dd} - S_{dc})(1 - S_{cc} - S_{cd})}{(1 - S_{dd} - S_{cd})(1 - S_{cc} + S_{cd})} \right). \quad (23)$$

Likewise  $\Gamma_d$ , in some cases, (23) can lead to an indetermination if it is directly developed. In order to avoid such indetermination,  $Z_d$  can be naturally split into two cases: 1) the two-port is ideally symmetric, which means that the second term in (23) can be simplified since  $S_{cd} = S_{dc} = 0$ ; 2) otherwise (even when designing the device as a differential component). Therefore,  $Z_d$  is expressed as follows

$$Z_d = \begin{cases} 2Z_0 \frac{1 + S_{dd}}{1 - S_{dd}} & \text{if } S_{dc} = S_{cd} = 0 \\ 2Z_0 \frac{S_{dd} - S_{cc} + 1 - |S|}{1 + |S| - S_{dd} - S_{cc}} & \text{Otherwise} \end{cases}. \quad (24)$$

As it was expected,  $Z_d$  matches  $Z_{dd}$  only when the two-port is symmetric. It can be seen that, the same result is obtained by applying the bilinear transformation (16) to (15). Therefore, the former theory is consistent with circuit theory.

### 3.3. $\Gamma_c$ when $\Gamma_L^d=1$

Replacing  $\Gamma_L^d = 1$  in (10),  $\Gamma_c$  results as follows

$$\Gamma_c = \frac{S_{cc} - |S|}{1 - S_{dd}}. \quad (25)$$

Also in this case, when the device is purely balanced and floating (i.e.,  $S_{dd} = 1$  and  $|S| = S_{cc}$ ), (25) results in an indetermination. This indetermination is naturally solved by using (10) and  $\Gamma_c$  results in  $S_{cc}$ . If the device is simply symmetric and non-mode conversion is allowed, (i.e.,  $S_{dc} = S_{cd} = 0$ ),  $\Gamma_c$  results in  $S_{cc}$ .

Moreover, when  $\Gamma_L^d = 1$  and (18) are inserted in (11), it is obtained that  $I_1 = I_2$ . Then, the normalized power waves can be replaced by two equivalent current sources connected at both ports as it is shown in Fig. 5. This equivalent driving condition is also consistent if one realizes that no differential current is allowed, thus from the point of view of the differential-mode, this boundary condition is seen as an open circuit.

In order to calculate  $Z_c$ , (25) is substituted in the following bilinear transformation

$$Z_c = \frac{Z_0}{2} \frac{1 + \Gamma_c}{1 - \Gamma_c}. \tag{26}$$

Therefore the common-mode impedance  $Z_c$  when  $\Gamma_L^d = 1$  results

$$Z_c = \begin{cases} \frac{Z_0}{2} \frac{1 + S_{cc}}{1 - S_{cc}} & \text{if } S_{dc} = S_{cd} = 0 \\ \frac{Z_0}{2} \frac{S_{dd} - S_{cc} - 1 + |S|}{S_{dd} + S_{cc} - 1 - |S|} & \text{Otherwise} \end{cases}. \tag{27}$$

As expected, only in the case when the two-port is symmetric  $Z_c$  matches with  $Z_{cc}$ .

### 3.4. $\Gamma_d$ when $\Gamma_L^c = -1$

When  $\Gamma_L^c = -1$ ,  $\Gamma_d$  is given by

$$\Gamma_d = \frac{S_{dd} + |S|}{1 + S_{cc}}. \tag{28}$$

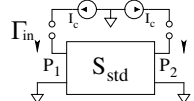
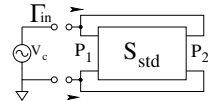
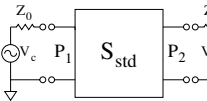
Again, if the device is purely symmetric (i.e.,  $S_{dc} = S_{cd} = 0$  and  $|S| = S_{dd}S_{cc}$ ),  $\Gamma_d$  results in  $S_{dd}$  as expected. It is also interesting to write (7) when  $\Gamma_L^c = -1$ ,

$$a_1 = -a_2 - \sqrt{2}b_c. \tag{29}$$

As it has been previously mentioned,  $a_1$  differs from  $-a_2$  except when the two port is purely symmetric. Otherwise, replacing  $b_c$  by (6) and by means of (18),  $V_1 = -V_2$ . Again, the power waves sources can be replaced by single-ended voltage sources as it is shown in Fig. 5. Notice from Fig. 5 that the common-mode node between the differential voltage sources is shorted, thus  $\Gamma_L^c = -1$ .

Thus,  $Z_d$  can be calculated replacing (28) in the impedance

	$\Gamma_L^c$	1	-1	0
	b.c.	$I_1 = -I_2$	$V_1 = -V_2$	$a_1 = -a_2$
$\Gamma_d$	Equivalent driving method			
	Expression	$\frac{S_{dd} -  S }{1 - S_{cc}}$	$\frac{S_{dd} +  S }{1 + S_{cc}}$	$S_{dd}$

$\Gamma_c$	$\Gamma_L^d$	1	1	0
	b.c.	$I_1 = I_2$	$V_1 = V_2$	$a_1 = a_2$
	Equivalent driving method			
	Expression	$\frac{S_{cc} -  S }{1 - S_{dd}}$	$\frac{S_{cc} +  S }{1 + S_{dd}}$	$S_{cc}$

**Figure 5.** Two-port mixed-mode driving topologies.

transformation (16),

$$Z_d = \begin{cases} 2Z_0 \frac{1 + S_{dd}}{1 - S_{dd}} & \text{if } S_{dc} = S_{cd} = 0 \\ 2Z_0 \frac{S_{dd} + S_{cc} + 1 + |S|}{1 - |S| - S_{dd} + S_{cc}} & \text{Otherwise} \end{cases} \quad (30)$$

### 3.5. $\Gamma_c$ when $\Gamma_L^d = -1$

Replacing  $\Gamma_L^d = -1$  in (10),  $\Gamma_c$  reads as

$$\Gamma_c = \frac{S_{cc} + |S|}{1 + S_{dd}} \quad (31)$$

Likewise in the previous cases, when the device is symmetric (i.e.,  $S_{dc} = S_{cd} = 0$  and  $|S| = S_{dd}S_{cc}$ ),  $\Gamma_c$  results in  $S_{cc}$ . Once more, rewriting (11) when  $\Gamma_L^d = -1$ ,

$$a_1 = a_2 - \sqrt{2}b_d \quad (32)$$

As it has been previously mentioned,  $a_1$  differs from  $a_2$  except when the two port is purely symmetric. Otherwise, replacing  $b_d$  by (6) and by means of (18),  $V_1 = V_2$ . In this case, the power waves can be replaced by a voltage source connected to both ports as in Fig. 5. Therefore, any differential voltage source has been shorted; it implies that from the point of view of the differential-mode,  $\Gamma_L^d$  equals  $-1$ .

A new expression for  $Z_c$  can be calculated replacing (31) in (26),

$$Z_c = \begin{cases} \frac{Z_0}{2} \frac{1 + S_{cc}}{1 - S_{cc}} & \text{if } S_{dc} = S_{cd} = 0 \\ \frac{Z_0}{2} \frac{S_{dd} + S_{cc} + 1 + |S|}{1 - |S| + S_{dd} - S_{cc}} & \text{Otherwise} \end{cases} \quad (33)$$

At this point, a set of different expressions for  $\Gamma_d(\Gamma_c)$  and  $Z_d(Z_c)$  have been obtained through driving a two-port device with

different standard mixed-mode loads. As it has been previously shown, these expressions can be applied to non-symmetrical two-port devices. However, it is important to notice that each of these expressions are only valid for a specific boundary conditions which are summarized in Fig. 5.

#### 4. PRACTICAL CASE

An integrated inductor can be considered as a two-port device similar to the one on Fig. 2. Thus, the former theory can be applied to the evaluation of the quality factor,  $Q$ , of inductors.  $Q$  is defined as a ratio of the stored reactive energy over the energy loss evaluated in one cycle. However, this definition is quite subtle because the stored energy is actually dependent on the shape of electromagnetic fields around the component. These fields are related to the geometry, including layout elements nearby; but, most important, to the way in which the inductor is excited in [21–23]. Noticing the benefit of exciting inductors differentially, Rabjohn introduced the use of symmetrical shapes in the implementation of fully differential RFICs substituting traditional spiral ones [24, 25]. Thus, for any inductor,  $Q$  is given by

$$Q = \frac{\text{Im} \{Z_d\}}{\text{Re} \{Z_d\}}, \quad (34)$$

where, as demonstrated previously, for an ideal symmetric inductor  $Z_d$  results in  $Z_{dd}$ . However, even though a symmetrical shape is used in their implementation, symmetry is not always guaranteed. Indeed, cross-bridges sections or layout asymmetries at the surrounding area of an inductor can break the symmetry of its own electromagnetic fields. Furthermore, there is still many situations in which spiral inductors can be preferred over symmetrical ones, e.g., when one of the terminal of the inductor is grounded, or when area reduction prevails over symmetry [26, 27]. For these cases, the choice between symmetric and spiral topologies is currently set through the comparison of the  $Q$  factor when driving the device differentially. Thereby, it is important to find the correct definition of  $Q$  for both topologies, i.e., it must be avoided that any inductor shape benefits itself from the definition of the  $Q$  factor. To proceed with, the previously developed theory and concepts provide a correct framework for such comparison.

Figure 6 shows two inductors using different topologies, symmetric and spiral, that have been synthesized using layout optimization techniques [28] for a given application in the frequency range of 2.45GHz using a 0.35  $\mu\text{m}$  CMOS technology. Their geometrical characteristics are summarized in Table 1. Notice that both geometries

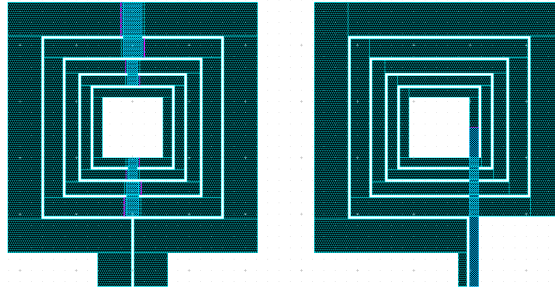


**Figure 6.** Symmetric and spiral optimized inductors layout.

**Table 1.** Geometrical characteristics of both inductors.

Number of turns	5
Inner diameter [ $\mu\text{m}$ ]	54
Spacing between turns [ $\mu\text{m}$ ]	2.5
Width of the first turn (inner turn) [ $\mu\text{m}$ ]	7.8
Width of the second turn [ $\mu\text{m}$ ]	8.6
Width of the third turn [ $\mu\text{m}$ ]	11.1
Width of the fourth turn [ $\mu\text{m}$ ]	16.8
Width of the fifth turn (outer turn) [ $\mu\text{m}$ ]	30

are quite similar, thus a similar  $Q$  factor behavior should be expected. Both layouts have been simulated with MoMentum, a planar solver from Agilent Technologies, obtaining the two-port single-ended  $S$ -parameter matrix over a frequency range beyond the Self Resonance Frequency (SRF). The obtained  $S$ -parameters are later mathematically converted to mixed-mode  $S$ -parameters matrix description [6].

When exciting symmetric inductors differentially, non reflected common-mode power wave exist which means that the response of the component is independent of the common-mode load  $\Gamma_L^c$ , as it has been previously demonstrated. Then,  $Z_d$  equals  $Z_{dd}$  and (2) and (34) are equivalent. Fig. 7 shows a plot of the  $Q$  factor value for the previous given symmetrical inductor when loaded with  $\Gamma_L^c = 0, 1$  and  $-1$ . As expected, all the cases give the same  $Q$  factor behavior.

On the contrary, the differential excitation of a spiral inductor allows the existence of a common-mode reflected power wave. Therefore, the response of the device is dependent on the value of the common-mode load  $\Gamma_L^c$ . Using the same common-mode load conditions as in the previous symmetrical case (i.e., open, short and match), Fig. 8 shows the behavior of  $Q$  for the non-symmetric inductor. It is worth

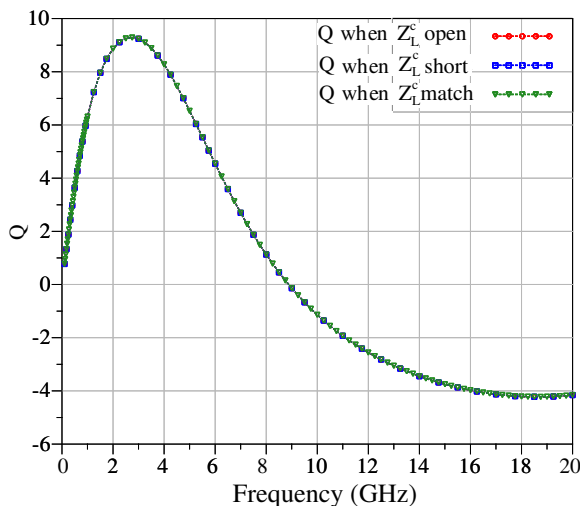


**Figure 7.** Quality factor vs. frequency for a symmetric inductor using (34) when  $Z_L^c = Z_0/2$  (match), open, short.

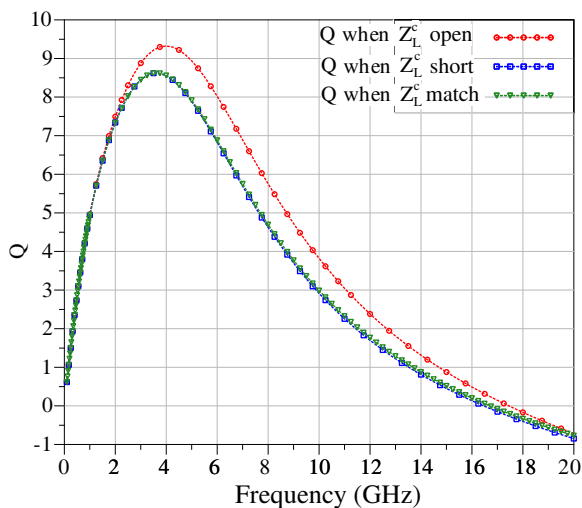


**Figure 8.** Quality factor vs. frequency for an asymmetric inductor using (34) when  $Z_L^c = Z_0/2$  (match), open, short.

noting that differences larger than a 10% can be obtained depending on the boundary condition, i.e., the value of  $Q$  can be boosted just because of the definition of  $Q$  itself. Therefore, once an inductor is chosen, the main issue is to identify the correct boundary conditions which lead to the adequate value of  $Q$ .

## 5. CONCLUSIONS

The theory of mixed-mode scattering parameters has been extended not only to symmetrical devices, but to non-symmetrical or actual devices, finding a general expression for  $\Gamma_d(\Gamma_c)$  that resembles the well-known expressions of  $\Gamma_{in}(\Gamma_{out})$  for a single-ended two-port device. It has also been shown that the former particular cases of the driving of a two-port device are reduced to the application of a short, open and matched mixed-mode load conditions on the general expression of  $\Gamma_d(\Gamma_c)$ . Moreover, such definitions allow to obtain  $Z_d(Z_c)$  in terms of  $S_{mm}$ . An analytic connection between scattering-parameters description in both versions, through the use of  $S$ -parameters and  $S_{mm}$ , and lumped elements description has naturally been used toward the consecution of these expressions. As a practical case, the  $Q$  value for symmetrical and non-symmetrical inductors has been obtained using the definition of  $Z_d$ , illustrating the differences when considering different boundary conditions.

## ACKNOWLEDGMENT

This work was supported in part by the Spanish Ministry of Innovation and Science (with support from the European Regional Development Fund) under contract TEC2010-14825/MIC and TEC2010-21484; and in part by the Andalusian Regional Council of Innovation, Science and Enterprise under contract TIC-2532 and with the support of the Department of University, Research and society of information of Government of Catalonia. T. Carrasco would like to thank Prof. Mohammed Ismail from Ohio State University, for his warm hospitality during his visit to the ElectroScience Laboratory in OSU.

## REFERENCES

1. Amin, Y. and H. Tenhunen, "Development and analysis of exible UHF RFID antennas for "green" electronics," *Progress In Electromagnetics Research*, Vol. 130, 1–15, 2012.
2. Wu, S.-M., C.-T. Kuo, P.-Y. Lyu, Y. L. Shen, and C.-I. Chien, "Miniaturization design of full differential bandpass filter with coupled resonators using embedded passive device technology," *Progress In Electromagnetics Research*, Vol. 121, 365–379, 2011.
3. Bockelman, D. E. and W. R. Eisenstadt, "Combined differential and common-mode scattering parameters: Theory and simulation," *IEEE Transactions on Microwave Theory and Techniques*, Vol. 43, No. 7, 1530–1539, Jul. 1995.



4. Bockelman, D. E. and W. R. Eisenstadt, "Combined differential and common-mode analysis of power splitters and combiners," *IEEE Transactions on Microwave Theory and Techniques*, Vol. 43, No. 11, 2627–2632, Nov. 1995.
5. Skyworks Application Note, "Matching differential port device," Skyworks Solutions, Inc., Oct. 2009.
6. Danesh, M., "Monolithic inductors for silicon radio frequency integrated circuits," M. A. Sc. Thesis, Dept. Elect. Comput. Eng., Univ. Toronto, Toronto, ON, Canada, 1999.
7. Danesh, M. and J. R. Long, "Differentially driven symmetric microstrip inductors," *IEEE Transactions on Microwave Theory and Techniques*, Vol. 50, No. 1, 332–341, Jan. 2002.
8. Kuo, S. K., S. L. Chen, and C. T. Lin, "An accurate method for impedance measurement of RFID tag antenna," *Progress In Electromagnetics Research*, Vol. 83, 93–106, 2008.
9. Danesh, M. and J. R. Long, "Authors' reply," *IEEE Transactions on Microwave Theory and Techniques*, Vol. 55, No. 4, 809–810, Apr. 2007.
10. Meys, R. and F. Janssens, "Measuring the impedance of balanced antennas by an  $S$ -parameter method," *IEEE Antennas and Propagation Magazine*, Vol. 40, No. 6, 62–65, Dec. 1998.
11. Qing, X. and Z. N. Chen, "Impedance characterization of RFID tag antennas and application in tag co-design," *IEEE Transactions on Microwave Theory and Techniques*, Vol. 57, No. 5, 1268–1274, May 2009.
12. Konstroffer, L., "Finding the reflection coefficient of a differential one-port device," *RF Semiconductor*, 1999.
13. Drakaki, M., A. A. Hatzopoulos, and A. Siskos, "CMOS inductor performance estimation using  $Z$ - and  $S$ -parameters," *IEEE International Symposium on Circuits and Systems, ISCAS*, 2256–2259, 2007.
14. Collin, R. E., *Foundations for Microwave Engineering*, 2nd Edition, Wiley-IEEE Press, Dec. 2000.
15. Liang, C. H., Y. Shi, and T. Su, " $S$  parameters theory of lossless block network," *Progress In Electromagnetics Research*, Vol. 104, 253–266, 2010.
16. Wloczynski, S., "Match the ports of differential devices," *Microwaves and RF*, ED Online ID #22407 Edition, Feb. 2010.
17. Bockelman, D. E. and W. R. Eisenstadt, "Pure-mode network analyzer for on-wafer measurements of mixed-mode  $S$ -parameters of differential circuits," *IEEE Transactions on Microwave Theory*

- and Techniques*, Vol. 45, No. 7, 1071–1077, Jul. 1997.
18. Zwick, T. and U. R. Pfeiffer, “Pure-mode network analyzer concept for on-wafer measurements of differential circuits at millimeter-wave frequencies,” *IEEE Transactions on Microwave Theory and Techniques*, Vol. 53, No. 3, 934–937, Mar. 2005.
  19. Qing, X. and Z. N. Chen, “Comments on ‘measuring the impedance of balanced antennas by an  $S$ -parameter method’,” *IEEE Antennas and Propagation Magazine*, Vol. 52, No. 1, 171–172, Feb. 2010.
  20. Kaldjob, E., B. Geck, and H. Eul, “Comments on ‘measuring the impedance of balanced antennas by an  $S$ -parameter method’,” *IEEE Antennas and Propagation Magazine*, Vol. 50, No. 6, 113–114, Dec. 2008.
  21. Pan, S. J., L. W. Li, and W. Y. Yin, “Performance trends of on-chip spiral inductors for RFICs,” *Progress In Electromagnetics Research*, Vol. 45, 123–151, 2004.
  22. Carrillo, T. C., J. G. Macias-Montero, A. O. Marti, J. S. Cordoba, and J. M. Lopez-Villegas, “CMOS single-ended-to-differential low-noise amplifier,” *Integration, the VLSI Journal*, Vol. 42, No. 3, 304–311, 2009, Special Section on DCIS2006.
  23. Aluigi, L., F. Alimenti, and L. Roselli, “Automatic design and 3D electromagnetic simulation of sub-nH spiral inductors,” *PIERS Proceedings*, 1719–1722, Marrakesh, Morocco, Mar. 20–23, 2011.
  24. Rabjohn, G. G., “Monolithic microwave transformers,” M. Eng. Thesis, Carleton University, Ottawa, ON, Canada, Apr. 1991.
  25. Zheng, Y. and C. E. Saavedra, “Frequency response comparison of two common active inductors,” *Progress In Electromagnetics Research Letters*, Vol. 13, 113–119, 2010.
  26. Abdullah, E., “Planar inductor design for high power applications,” *Progress In Electromagnetics Research B*, Vol. 35, 53–67, 2011.
  27. Wang, R., J. Xu, C.-L. Wei, M.-Y. Wang, and X.-C. Zhang, “Improved extraction of coupling matrix and unloaded  $Q$  from  $S$ -parameters of lossy resonator filters,” *Progress In Electromagnetics Research*, Vol. 120, 67–81, 2011.
  28. Lopez-Villegas, J. M., J. Samitier, C. Cane, P. Losantos, and J. Bausells, “Improvement of the quality factor of RF integrated inductors by layout optimization,” *IEEE Transactions on Microwave Theory and Techniques*, Vol. 48, No. 1, 76–83, Jan. 2000.